Effects of Complexing Agents on Three Steps Pulse Electrodeposited SnS Thin Films

A. Supee[1,2,*], Y. Tanaka[2], M. Ichimura[2]

1. Faculty of Petroleum and Renewable Energy Engineering (FPREE), Universiti Teknologi Malaysia, 81310 Johor Bahru, Johor, Malaysia

2. Department of Engineering Physics, Electronics and Mechanics, Nagoya Institute of Technology, Gokiso, Showa, Nagoya 466-8555, Japan

* E-Mail: ichimura.masaya@nitech.ac.jp

ABSTRACT

SnS thin films were prepared on indium-tin-oxide-coated glass substrate at room temperature via three steps pulse electrodeposition from an aqueous bath containing 30 mM $SnSO_4$ and 100 mM $Na_2S_2O_3$. The effects of two complexing agents, i.e., ethylenediaminetetraacetic (acid-EDTA $[CH_2N(CH_2COOH)_2]_2$) and L(+)-tartaric acid ($C_4H_6O_6$) under different concentration were studied. All the deposited samples exhibited p-type conductivity behaviour. The films deposited with the complexing agents generally showed less oxygen content and larger sulfur content than those deposited without the agents. The film thickness was decreased by addition of EDTA and low concentration of tartaric acid (<10 mM), while it was slightly increased with a large amount of tartaric acid (>30 mM). Larger crystalline size and larger optical transmission were observed for SnS deposited with tartaric acid concentration larger than 30 mM.

Keywords: tin sulfide, complexing agents, electrodeposition

1. Introduction

Tin monosulphide (SnS) is an important IV-VI group semiconductor material occurring in nature as orthorhombic structure [1]. Owing to favorable optoelectronic properties and abundance of the constituent elements, there are growing interest in SnS as a promising novel absorber layer in fabrication of hetero-junction solar cells over the past decade. Its direct and indirect band gap are estimated to be 1.3-1.5 eV [2-6] and 1.0-1.1 eV [7-9] respectively, which are suitable for absorption of the solar radiation. Besides that, it also has high absorption coefficient ($\alpha > 10^4$ cm^{-1}) in the visible range [2-3, 6]. The theoretical conversion efficiency can reach up to 25% [10], and several research groups have achieved efficiencies larger than 2% [11-13].

Various methods have been applied to deposit SnS thin films such as vacuum evaporation [3, 14], sulfurization of Sn metal [15], chemical bath deposition [16], spray pyrolysis [6] and electrodeposition (ED) [17-18]. Among them, ED has the advantages of being non-vacuum, economic, capable of large scale deposition, and several experimental parameters can be controlled easily. The deposition potential in ED process also can be manipulated, and the conventional deposition modes used are galvanostatic (constant current) and potentiostatic (constant potential). In addition, the potential can be modulated with two-step or three-step pulse. In previous works, it was found that the surface morphology and photosensitivity of SnS thin film were highly improved by adopting three steps pulse ED [19].

In the SnS ED method, common type of solution used is tin (II) sulfate ($SnSO_4$) and sodium thiosulfate ($Na_2S_2O_3$) with addition of sulfuric acid (H_2SO_4) or hydrochloric acid (HCl) to adjust the pH. The quality of the deposited SnS film strongly relies on the electrolyte's composition used. The use of complexing agents is common in ED of metals and is thought to improve electrolyte stability, produce sufficient adherence and smooth microstructure. For ED of SnS also, it was reported that the complexing agents can make the composition more stoichiometric [20-21].

In this work, we carry out three steps pulse ED of SnS thin films with two different complexing agents, i.e., ethylenediaminetetraacetic acid (EDTA $[CH_2N(CH_2COOH)_2]_2$) and L(+)-tartaric acid ($C_4H_6O_6$). So far, effects of those complexing agents have been studied only for galvanostatic and DC potentiostatic ED of SnS [20-22]. In addition, no comparison has

been done for the effects of both EDTA and tartaric acid on SnS ED. Hence, in this paper, we discuss the effects of EDTA and tartaric acid on the three steps pulse ED SnS film properties in terms of cyclic voltammetry (CV), thickness, surface morphology, composition ratio, crystalline structure, optical transmission, and photoresponse. The SnS film without complexing agents is set as the control sample, and the effects of different concentrations of complexing agents are compared.

2. Experiments

A conventional three electrode cell was used in ED with indium-tin-oxide (ITO)-coated glass substrate with resistivity of 10 Ω/cm^2 as the working electrode (WE), a platinum sheet as the counter electrode (CE) and a saturated calomel electrode (SCE) as the reference electrode (RE). The deposition area was fixed to 1 cm x 1 cm by masking and total deposition time was set to 7 minutes. Basic electrolyte solution contained 30 mM $SnSO_4$ and 100 mM $Na_2S_2O_3$ for the control sample, and different concentrations of the complexing agents ranging from 1 mM to 200 mM were added to the basic solution. However, for EDTA, it was limited to 10 mM due to the EDTA solubility limit in the solution. ED was performed using periodic three step pulse (potential: V_1 = -1 V vs SCE, on time t_1 = 10 s; V_2 = -0.6 V, t_2 = 10 s; V_3 = 0 V, t_3 = 10 s) at room temperature. Prior to each deposition, WE was cleaned using alkyl benzene and acetone, and rinsed with DI water. Meanwhile, CE was dipped into 30 ml sulfuric acid for 5 seconds, followed by ultrasonically rinsed with DI water. The pH of the electrolytes were not adjusted. Initial pH of the electrolytes were as follows: SnS (control): 2.71, SnS with EDTA 1 mM: 2.61, 3 mM: 2.58, 5 mM: 2.53, 10 mM: 2.21, SnS with tartaric acid: 1 mM: 2.54, 3 mM: 2.34, 5 mM: 2.31, 10 mM: 2.20, 30 mM: 1.83, 50 mM: 1.69, 100 mM: 1.56, 150 mM: 1.43, 200 mM: 1.39. After ED process was completed, WE was cleaned with steady stream of DI water and then dried using N_2 gas.

The deposition and CV measurement were conducted using potentiostat/galvanostat HA-151B and function generator HB-305 (Hokuto Denko). In CV, the potential was swept from 0 V to -1.5 V followed by -1.5 V to 0.5 V and finally from 0.5 V to 0 V at 20 mV/s. Optical transmittance was measured in the range of 300 nm to 1500 nm wavelength using V-570 UV/VIS/NIR spectrophotometer (JASCO). Film thicknesses were measured by a profile

meter Surfcom-1400D (Accretech-Tokyo Seimitsu). Surface morphology and compositional analysis were conducted using JAMP-9500F field emission Auger microprobe (JEOL) at a probe voltage of 10 keV and a current of $1x10^{-8}$ A. X-ray diffraction (XRD) patterns were recorded by SmartLab X-ray diffractometer (Rigaku) using a CuKα radiation source. Photoelectrochemical (PEC) measurements were carried out in an aqueous electrolyte containing 100 mM $Na_2S_2O_3$ under negative (0 V to -1 V) and positive (0 V to 1 V) potential scan. An Xenon lamp (80 mW/cm^2) was used as a source of light. The applied voltage was swept at 5 mV/s and the illumination was alternately switched on and off for each 5 s. All the characterization equipments mentioned above were operated at room temperature.

3. Results

Figures 1 (a) illustrates CV for the SnS control sample, SnS with EDTA and low concentration (up to 10 mM) of tartaric acid. In Fig. 1 (a), all the samples show clear anodic and cathodic peaks, and in the range of 0 V to about -0.60 V, there is no visible negative current appeared. Small shift of the cathodic peaks are observed, but the cathodic current density and curve shape are similar for all the samples.

The CV behaviours under high concentrations of tartaric acid (100 mM and 200 mM) were depicted in Figure 1 (b). Unlike Fig.1 (a), there is no visible cathodic current peaks observed, i.e., the cathodic current increased monotonically, and the anodic peaks shifted to a more negative potential compared to the control SnS solution. A curve shape similar to that of the control SnS was obtained by lowing pH to 1.54, with a minor anodic peak shift towards a more negative potential. However, the negative current is still lower than in the case of the high tartaric acid concentration. Thus, it can be conclude that the negative current was enhanced by addition of high tartaric acid concentration in the SnS deposition solution.

Figure 2 shows the potential and current profile during the deposition. Compared with the control SnS deposition (Fig.2(a)), there is no significant change in the profiles for the depositions with 10 mM EDTA (Fig.2(b)), 10 mM tartaric acid (Fig.2(c)) and 100 mM tartaric acid (Fig.2(d)), although the positive current is smaller for the deposition with 10 mM EDTA. On the other hand, the positive current decreased significantly during the deposition when 100 mM tartaric acid was added.

Table 1 summarized the thickness measured for the deposited samples. Addition of low concentrations of both the complexing agents caused in thickness reduction compared to the SnS control sample. However, thicker SnS films were produced under high tartaric acid concentration (from 30 to 100 mM). Further increase in tartaric acid concentration exceeding 100 mM resulted in small film thickness reduction. The colour of the films also changed from dark brown (control SnS and SnS with low concentrations of EDTA or tartaric acid) to the dark grey (high tartaric acid concentration).

Figures 3 (a)-(f) show the selected scanning electron microscope (SEM) images for the deposited samples. The SnS control sample exhibited relatively large flower-like agglomerates of grains occurring on its surface. Increase in EDTA and tartaric acid concentration from 1 mM to 10 mM lead to reduced compactness of the grains, as can be seen in Figure 3 (c) and (e). Further increased in tartaric acid concentration up to 100 mM resulted in more dense agglomeration grains with more well defined boundaries.

Figure 4 illustrates Auger electron spectra (AES) for the SnS control sample. S/Sn and O/Sn ratios were calculated using a commercially available standard SnS chemical as the reference sample and are plotted in Figs. 5 (a) and (b). The oxygen content was reduced with increasing EDTA and tartaric acid concentration. The oxygen content was further decreased when the tartaric acid concentration was greater than 10 mM as shown in Figure 5 (b). For the tartaric acid concentration greater than 50 mM, oxygen content was being constant and no further reduction occurred.

The sulfur content was also affected by the complexing agents concentration. Overall trends in Figs. 5 (a) and (b) exhibit increasing sulfur content with increasing EDTA and tartaric acid concentration. These results show similarity with the previous works conducted [1, 20-21].

Figure 6 depicts XRD results for the selected deposited samples and ITO-coated glass substrate. The peaks for the deposited samples were compared with PDF card (00-039-0354), and the orthorhombic SnS peaks appear at $2\Theta = 31.97°$ for (040) and/or $2\Theta = 31.53°$ for (111). For the sample deposited with 100 mM tartaric acid, the SnS peak seems to be sharper than those of the others and be shifted to a lower angle: the peak is thought to be dominantly due to

(111) diffraction rather than (040) diffraction. The small peak width indicates better crystallinity (larger crystalline grain size).

The optical transmittance were shown in Figs. 7 (a)-(d). The transmission of the control SnS is low even in the IR range, and an absorption edge was not observed. The transmission was increased by addition of the complexing agents. However, for the samples deposited with EDTA and with 1-10 mM tartaric acid, the film thickness is much smaller than the control SnS sample, and thus the enhanced transmission will be mainly due to the reduced thickness. On the other hand, for the samples deposited with 30-200 mM tartaric acid, the thickness is comparable to or larger than that of the control sample, and still the transmission is significantly higher.

Clear optical transition slope was found in the samples deposited with 10 mM EDTA, and those with tartaric acid (greater than 3 mM), and thus the direct bandgap was estimated for them by the plot of $(\alpha h\nu)^2$ vs. $h\nu$, where α is the absorption coefficient and $h\nu$ the photon energy. The examples of the plot are shown in Fig. 8. The obtained bandgap values are listed in table 1. The bandgap for the sample with 10 mM EDTA was evaluated to be 1.58 eV, which is in agreement with those of SnS films deposited with EDTA under DC potential [21]. On the other hand, for the SnS samples with tartaric acid, the bandgap was in the range of 1.32 eV to 1.57 eV, different from those in the previous report of ED with tartaric acid. Bandgap energy estimated by the previous researcher for SnS with 200 mM tartaric acid was 1.05 eV and 1.09 eV when deposited at 70 ºC and 90 ºC, respectively [22].

Figure 9 depicts the photocurrent response in the PEC measurement for the SnS control sample under negative and positive voltage scan. The negative voltage scan exhibits larger photocurrent response compared to the positive voltage scan. As the sample was illuminated, the current was increased, and then decreased as the illumination was interrupted. All the other tested samples (not shown here) exhibit similar photocurrent response as the SnS control sample. This indicates that the electron is the minority carrier in the samples, since the current due to the minority carrier is enhanced by the illumination more significantly than the majority carrier current. Thus, it can be conclude that all the samples are photoactive and classified as p-type semiconductor.

For obtaining better understanding of photocurrent response for the tested samples, the difference between illuminated current (Ii) and dark current (Id) values at -0.80 V (negative voltage scan) and 0.50 V (positive voltage scan) were obtained. The difference was plotted against complexing agent concentration as shown in Figs 10 (a), (b) and (c). At -0.80 V, low concentration of both EDTA and tartaric acid (up to 10 mM) contributed to the larger photocurrent response compared to SnS control sample. This can partly be due to the decrease in the film thickness; since the sample is illuminated from the substrate side during the PEC measurement, a larger number of photons can reach the electrolyte/SnS interface with decreasing thickness. At higher tartaric acid concentration (30-200 mM), the negative response was smaller than for the control SnS as depicted in Fig. 10 (b), which would be due to a larger film thickness.

At 0.50 V, the samples deposited with both the complexing agents resulted in smaller photocurrent response than the SnS control sample, as shown in Fig. 10 (c). As noted above, the negative photoresponse of the samples deposited with the complexing agents is larger than or comparable to that of the control sample. Since dominance of negative response is characteristic of p-type semiconductors, those results indicate that SnS tends to have clearer p-type character with addition of the complexing agents.

4. Discussion

In ED, complexing agents are generally expected to form complex with metal ions and prevent formation of precipitation (e.g., metal hydroxide) or other spontaneous reactions in the solution. In ED of SnS, it was claimed in the previous works that the complex formation results in retardation of Sn deposition [20-21]. Then, deposition of elemental Sn metal is suppressed, and stoichiometric SnS can be obtained. In this work, with addition of EDTA or tartaric acid, the S/Sn ratio was increased as shown in Fig. 5. This will be due to the suppression of the Sn metal deposition by the complex formation. In addition, the O/Sn was decreased by the complexing agent, which could be due to the suppression of formation of $Sn(OH)_2$. However, in the case of EDTA and low concentration of tartaric acid, the deposition rate was significantly reduced. This is also thought to be due to the retardation of reduction of Sn ions. On the other hand, in the CV results, the negative current peak was not significantly

influenced by EDTA or low concentration of tartaric acid. In the current profile shown in Fig. 2, the current profile was not influenced significantly by EDTA and low concentrations of tartaric acid, although the thickness was decreased. Apparently, with the low concentrations of the complexing agents in the solution, the negative current was consumed for reactions other than SnS deposition, such as H_2S generation.

When the tartaric acid concentration was increased to 30 mM or more, the CV and deposition results are quite different from the low concentration case. In the previous work, it was found that with 200 mM tartaric acid in the solution, the dominant current contributor is sulfur species [22]. Thus, it seems that tartaric acid can retard Sn reduction and accelerate S reduction. Owing to formation of the reduced S species (S^{2-}, S^{-}), SnS could be formed by the reaction

$$Sn^{2+} + S^{2-} = SnS \qquad (1)$$

A small amount of SnS_2 and Sn_2S_3 may also be formed so that S/Sn can exceed unity, as shown in Fig. 5. The samples deposited with the high concentrations of tartaric acid showed a sharper XRD peak and higher optical transmission than the control sample. This will be due to the suppression of elemental Sn deposition. The reduction of the positive current in the current profile shown in Fig. 2 can also be due to decreased amount of elemental Sn, which can be dissolved during the positive pulse period more easily than the sulfides. Thus we may conclude that tartaric acid can generally improve the properties of SnS films. However, the acceleration of the S reduction by tartaric acid can be significant only when the tartaric acid concentration is comparable to that of the sulfur source, i.e., thiosulfate ion (100 mM). Thus, at the low concentration (<10 mM), only the retardation effect would be observed and the thickness was decreased.

4. Conclusion

SnS thin films have been prepared on ITO-coated glass substrate at room temperature via three steps pulse ED from an aqueous bath containing $SnSO_4$ and $Na_2S_2O_3$, and the effects of two complexing agents, EDTA and tartaric acid were studied. The films deposited with the complexing agents generally show less oxygen content and larger sulfur content than those deposited without the agents. The film thickness was decreased by addition of EDTA and low

concentration of tartaric acid (<10 mM), while it was slightly increased with a large amount of tartaric acid (>30 mM). Crystallinity and optical transmission were improved when tartaric acid concentration was larger than 30 mM. The effects of tartaric acid can be explained considering suppression of elemental Sn deposition and enhancement of sulfur reduction.

References

[1] A. Ghazali, Z. Zainal, M. Zobir Hussein, A. Kassim, Cathodic electrodeposition of SnS in the presence of EDTA in aqueous media, Sol. Energy Mater. Sol. Cells, 55 (1998) 237-249.

[2] M. Parenteau, C. Carlone, Influence of temperature and pressure on the electronic transitions in SnS and SnSe semiconductors, Phys. Rev. B, 41 (1990) 5227-5234.

[3] H. Noguchi, A. Setiyadi, H. Tanamura, T. Nagatomo, O. Omoto, Characterization of vacuum-evaporated tin sulfide film for solar cell materials, Sol. Energy Mater. Sol. Cells, 35 (1994) 325-331.

[4] P. Pramanik, P.K. Basu, S. Biswas, Preparation and characterization of chemically deposited tin(II) sulphide thin films, Thin Solid Films, 150 (1987) 269-276.

[5] R.H. Bube, Photoconductivity of solids, Wiley, New York, 1960 p. 233.

[6] N. Koteswara Reddy, K.T. Ramakrishna Reddy, Growth of polycrystalline SnS films by spray pyrolysis, Thin Solid Films, 325 (1998) 4-6.

[7] K. Takeuchi, M. Ichimura, E. Arai, Y. Yamazaki, SnS thin films fabricated by pulsed and normal electrochemical deposition, Sol. Energy Mater. Sol. Cells, 75 (2003) 427-432.

[8] S.C. Ray, M.K. Karanjai, D. DasGupta, Structure and photoconductive properties of dip-deposited SnS and SnS_2 thin films and their conversion to tin dioxide by annealing in air, Thin Solid Films, 350 (1999) 72-78.

[9] W. Albers, C. Haas, F. van der Maesen, The preparation and the electrical and optical properties of SnS crystals, J. Phys. Chem. Solids, 15 (1960) 306-310.

[10] K.T. Ramakrishna Reddy, P. Purandhara Reddy, P.K. Datta, R.W. Miles, Formation of polycrystalline SnS layers by a two-step process, Thin Solid Films, 403–404 (2002) 116-119.

[11] P. Sinsermsuksakul, L. Sun, S.W. Lee, H.H. Park, S.B. Kim, C. Yang, R.G. Gordon, Overcoming efficiency limitations of SnS-based solar cells, Adv. Energy Mater., 4 (2014) 1400496-1-7.

[12] P. Sinsermsuksakul, K. Hartman, S. Bok Kim, J. Heo, L. Sun, H. Hejin Park, R. Chakraborty, T. Buonassisi, R.G. Gordon, Enhancing the efficiency of SnS solar cells via band-offset engineering with a zinc oxysulfide buffer layer, Appl. Phys. Lett., 102 (2013) 053901-1-5.

[13] T. Ikuno, R. Suzuki, K. Kitazumi, N. Takahashi, N. Kato, K. Higuchi, SnS thin film solar cells with Zn1−xMgxO buffer layers, Appl. Phys. Lett., 102 (2013) 193901-1-4.

[14] B. Ghosh, M. Das, P. Banerjee, S. Das, Fabrication of vacuum-evaporated SnS/CdS heterojunction for PV applications, Sol. Energy Mater. Sol. Cells, 92 (2008) 1099-1104.

[15] K.T. Ramakrishna Reddy, P. Purandhara Reddy, Structural studies on SnS films grown by a two-stage process, Mater. Lett., 56 (2002) 108-111.

[16] D. Avellaneda, G. Delgado, M.T.S. Nair, P.K. Nair, Structural and chemical transformations in SnS thin films used in chemically deposited photovoltaic cells, Thin Solid Films, 515 (2007) 5771-5776.

[17] F. Kang, M. Ichimura, Pulsed electrodeposition of oxygen-free tin monosulfide thin films using lactic acid/sodium lactate buffered electrolytes, Thin Solid Films, 519 (2010) 725-728.

[18] S. Cheng, Y. Chen, Y. He, G. Chen, The structure and properties of SnS thin films prepared by pulse electro-deposition, Mater. Lett., 61 (2007) 1408-1412.

[19] K. Omoto, N. Fathy, M. Ichimura, Deposition of SnSxOy films by electrochemical deposition using three-step pulse and their characterization, Jpn. J. Appl. Phys., 45 (2006) 1500-1505.

[20] S. Cheng, Y. He, G. Chen, Structure and properties of SnS films prepared by electro-deposition in presence of EDTA, Mater. Chem. Phys., 110 (2008) 449-453.

[21] S. Cheng, Y. He, G. Chen, E.-C. Cho, G. Conibeer, Influence of EDTA concentration on the structure and properties of SnS films prepared by electro-deposition, Surf. Coat. Technol., 202 (2008) 6070-6074.

[22] J.R. Brownson, C. Georges, G. Larramona, A. Jacob, B. Delatouche, C. Lévy-Clément, Chemistry of tin monosulfide (δ-SnS) electrodeposition effects of pH and temperature with tartaric acid, J. Electrochem. Soc., 155 (2008) D40-D46.

Fig. 1. Cyclic voltammetry for SnS samples (a) SnS and low complexing agents concentration, and (b) SnS and high concentration of tartaric acid.

Fig. 2. Potential and current profiles during the deposition (a) SnS, (b) 10 mM EDTA, (c) 10 mM tartaric acid, and (d) 100 mM tartaric acid.

Fig. 3. SEM image of SnS deposited samples (a) SnS, (b) 3 mM EDTA, (c) 10 mM EDTA, (d) 3 mM tartaric acid, (e) 10 mM tartaric acid, and (f) 100 mM tartaric acid.

Fig. 4. AES for SnS control sample.

Fig. 5. (a) SnS and low concentration of complexing agents, and (b) SnS and high concentration of tartaric acid - Compositional analysis by AES.

Fig. 6. XRD patterns for selected deposited samples (a) ITO, (b) SnS, (c) 10 mM EDTA, (d) 10 mM tartaric acid, and (e) 100 mM tartaric acid.

Fig. 7. Optical transmittance of the deposited samples (a) SnS, (b) SnS with EDTA (low concentration), (c) SnS with tartaric acid (low concentration), and (d) SnS with tartaric acid (high concentration).

Fig. 8. $(\alpha hv)^2 \times 10^9$ ($cm^{-2}eV^2$) versus hv (eV) plot for the deposited samples.

Fig. 9. Photocurrent response in PEC measurement of SnS control sample.

Fig.10. (a) and (b) Comparison of the difference between the illuminated current and dark current (Ii-Id) of the tested samples at -0.8 V (negative voltage scan), (c) at 0.5 V (positive voltage scan).

Table 1. Thickness of the deposited films.

Type of deposited film	Complexing agent concentration (mM)	Thickness (μm)	Direct bandgap (eV)
SnS	0	0.25	-
SnS with EDTA	1	0.06	-
	3	0.04	-
	5	0.03	-
	10	0.03	1.58
SnS with Tartaric Acid	1	0.08	-
	3	0.05	-
	5	0.05	-
	10	0.05	1.51
	30	0.38	1.51
	50	0.50	1.57
	100	0.50	1.40
	150	0.30	1.35
	200	0.30	1.32

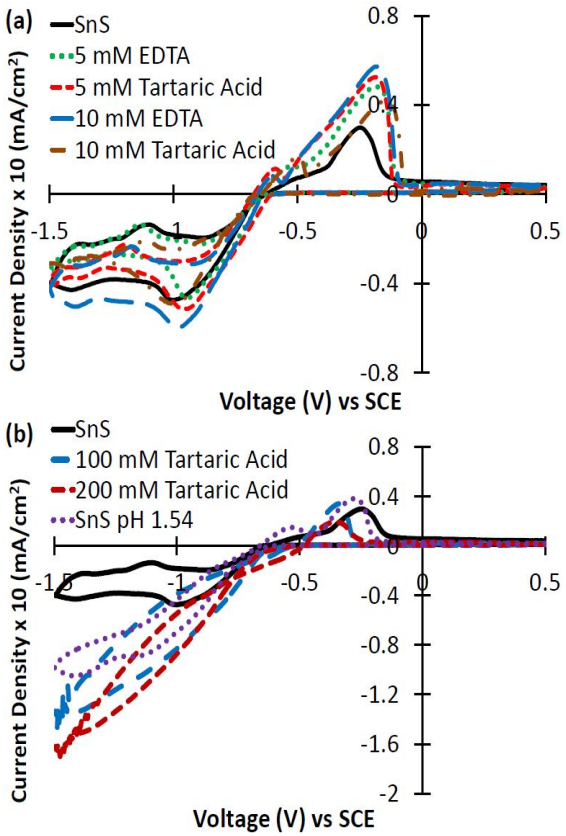

Fig. 1. Cyclic voltammetry for SnS samples (a) SnS and low complexing agents concentration, and (b) SnS and high concentration of tartaric acid.

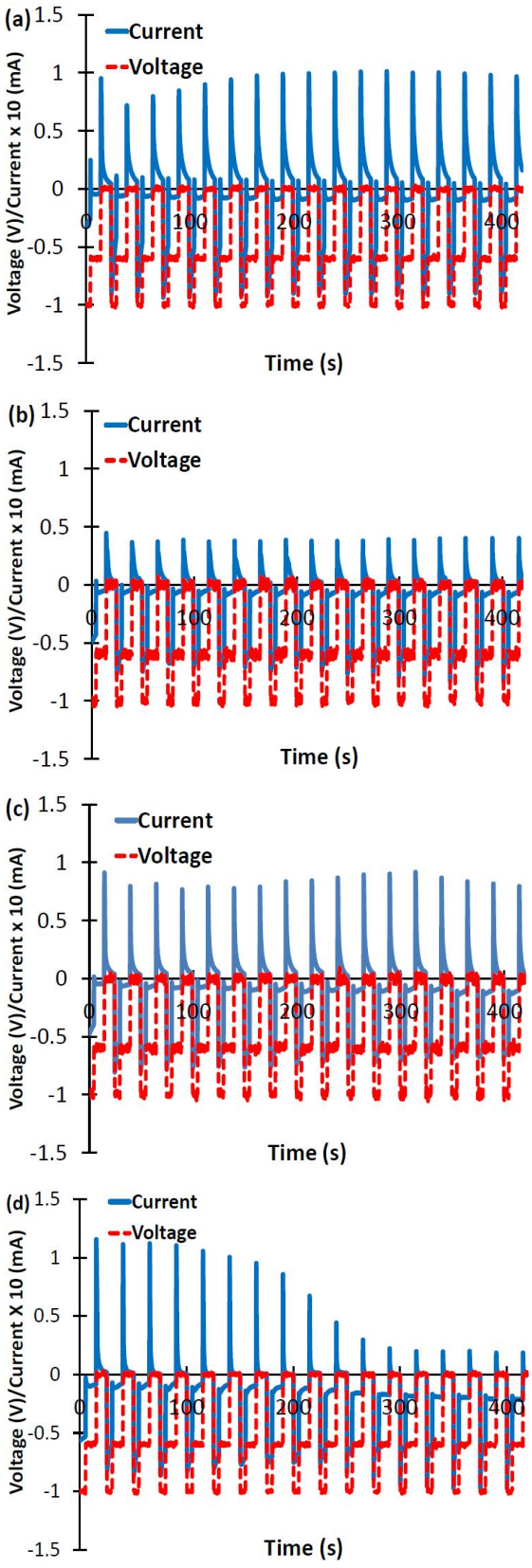

Fig. 2. Potential and current profiles during the deposition (a) SnS, (b) 10 mM EDTA, (c) 10 mM tartaric acid, and (d) 100 mM tartaric acid.

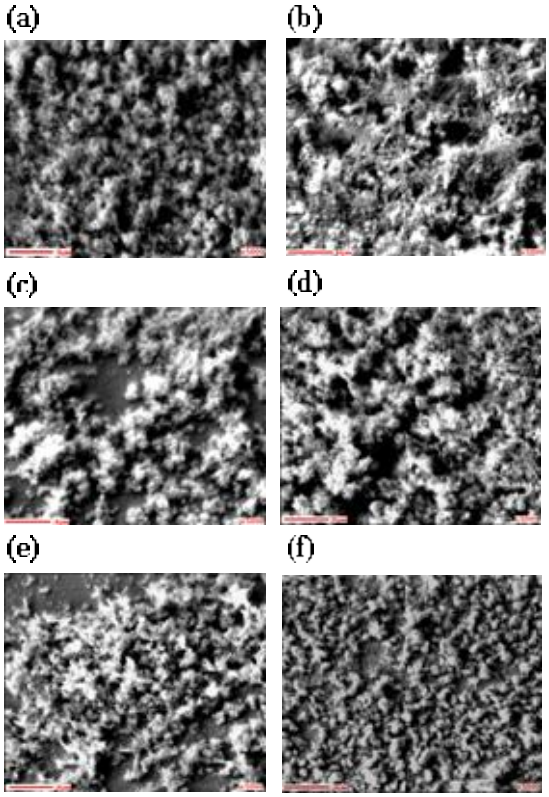

Fig. 3. SEM image of SnS deposited samples (a) SnS, (b) 3 mM EDTA, (c) 10 mM EDTA, (d) 3 mM tartaric acid, (e) 10 mM tartaric acid, and (f) 100 mM tartaric acid.

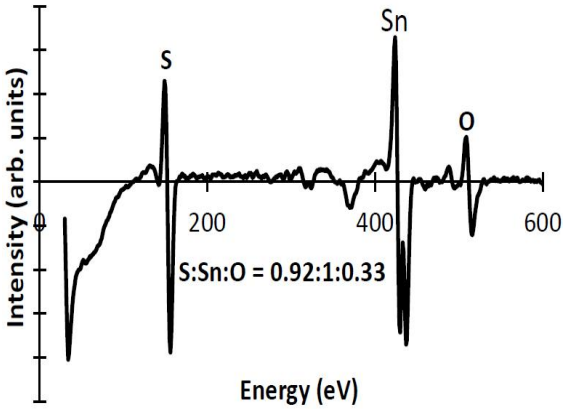

Fig. 4. AES for SnS control sample.

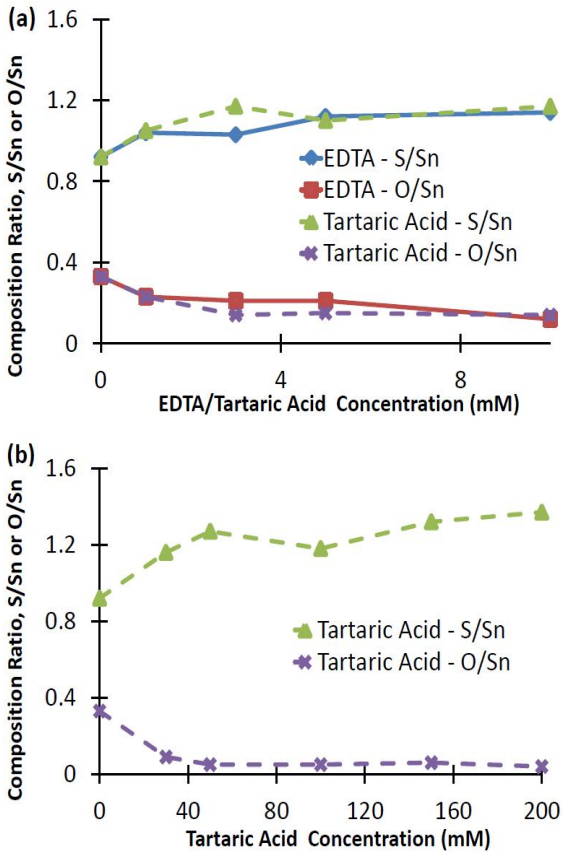

Fig. 5. (a) SnS and low concentration of complexing agents, and (b) SnS and high concentration of tartaric acid - Compositional analysis by AES.

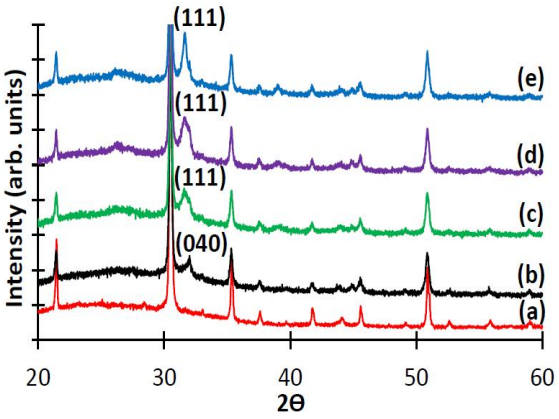

Fig. 6. XRD patterns for selected deposited samples (a) ITO, (b) SnS, (c) 10 mM EDTA, (d) 10 mM tartaric acid, and (e) 100 mM tartaric acid

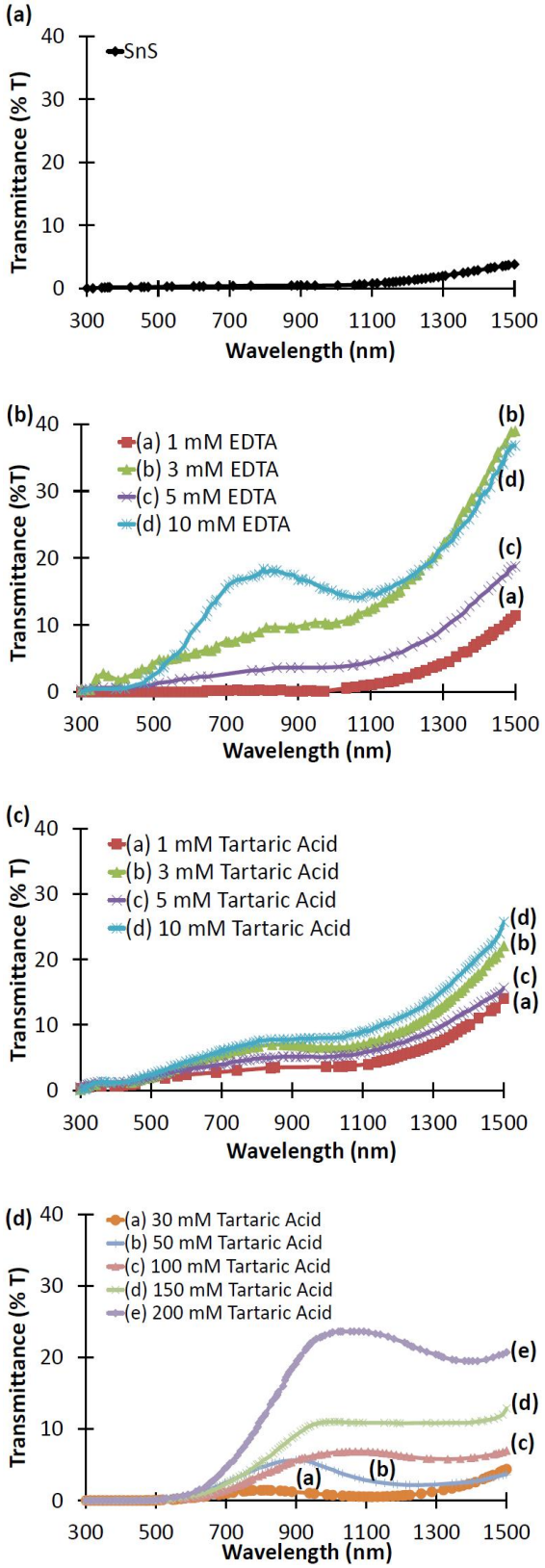

Fig. 7. Optical transmittance of the deposited samples (a) SnS, (b) SnS with EDTA (low concentration), (c) SnS with tartaric acid (low concentration), and (d) SnS with tartaric acid (high concentration).

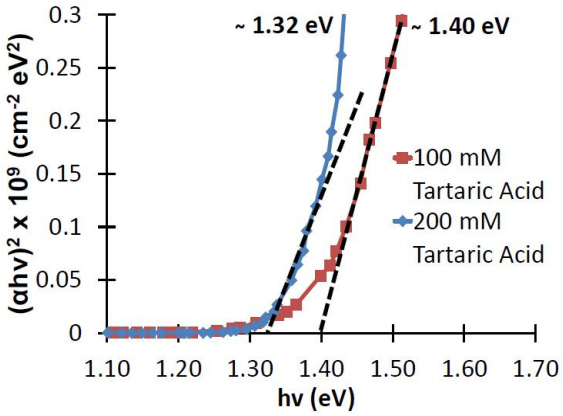

Fig. 8. $(\alpha hv)^2 \times 10^9$ ($cm^{-2}eV^2$) versus hv (eV) plot for the deposited samples.

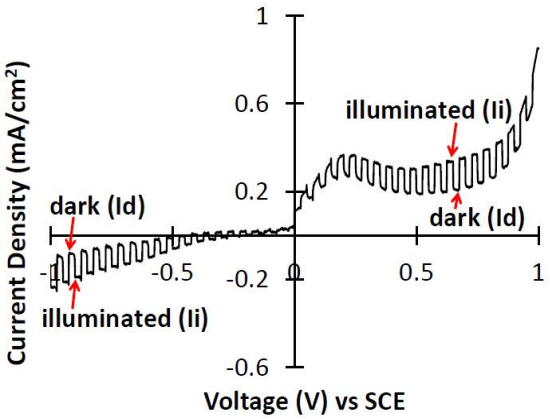

Fig. 9. Photocurrent response in PEC measurement of SnS control sample.

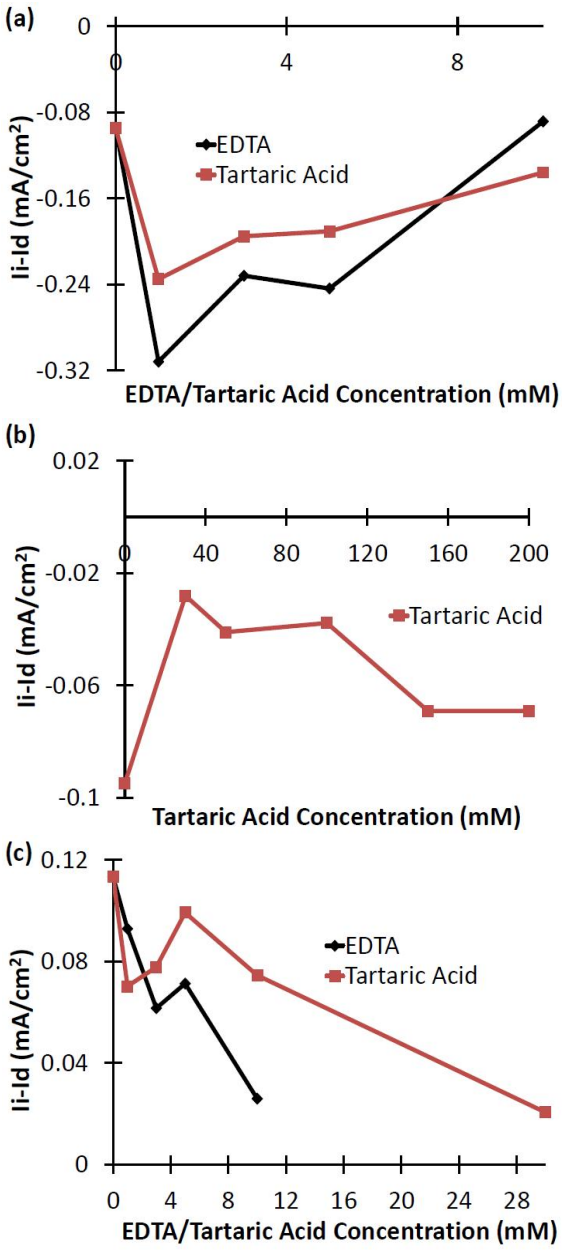

Fig.10. (a) and (b) Comparison of the difference between the illuminated current and dark current (Ii-Id) of the tested samples at -0.8 V (negative voltage scan), (c) at 0.5 V (positive voltage scan).